Efficient, D-glucose insensitive, growth on D-xylose by an evolutionary engineered Saccharomyces cerevisiae strain

Nijland, Jeroen G.; Li, Xiang; Shin, Hyun Yong; de Waal, Paul P.; Driessen, Arnold J. M.

Published in:
Fems Yeast Research

DOI:
10.1093/femsyr/foz083

Publication date:
2019

Efficient, D-glucose insensitive, growth on D-xylose by an evolutionary engineered *Saccharomyces cerevisiae* strain

Jeroen G. Nijland[1], Xiang Li[2], Hyun Yong Shin,[1] Paul P. de Waal,[3] and Arnold J.M. Driessen[1,#]

[#] Corresponding author: E-mail: a.j.m.driessen@rug.nl

[1] *Molecular Microbiology and Molecular Systems Biology*[2]*, Groningen Biomolecular Sciences and Biotechnology, University of Groningen, Zernike Institute for Advanced Materials and Kluyver Centre for Genomics of Industrial Fermentation, Groningen, The Netherlands*

[3] *DSM Biotechnology Center, Alexander Fleminglaan 1, 2613 AX, Delft, the Netherlands*

ABSTRACT

Optimizing D-xylose consumption in *Saccharomyces cerevisiae* is essential for cost-efficient cellulosic bioethanol production. An evolutionary engineering approach was used to elevate D-xylose consumption in a xylose-fermenting *S. cerevisiae* strain carrying the D-xylose-specific N367I mutation in the endogenous chimeric Hxt36 hexose transporter. This strain carries a quadruple hexokinase deletion that prevents glucose utilization, and allows for selection of

improved growth rates on D-xylose in the presence of high D-glucose concentrations. Evolutionary engineering resulted in D-glucose-insensitive growth and consumption of D-xylose which could be attributed to glucose insensitive D-xylose uptake via a novel chimeric Hxt37 N367I transporter that emerged from a fusion of the *HXT36* and *HXT7* genes, and a down regulation of a set of Hxt transporters that mediate glucose sensitive xylose transport. RNA sequencing revealed the down-regulation of *HXT1* and *HXT2* which, together with the deletion of *HXT7*, resulted in a 21% reduction of the expression of all plasma membrane transporters genes. Morphological analysis showed an increased cell size and corresponding increased cell surface area of the evolved strain, which could be attributed to genome duplication. Mixed strain fermentation of the D-xylose-consuming strain DS71054-evo6 with the D-glucose consuming CEN.PK113-7D strain resulted in decreased residual sugar concentrations and improved ethanol production yields compared to a strain which sequentially consumes D-glucose and D-xylose.

Keywords: Sugar transport, D-xylose transporter, bioethanol, co-fermentation, yeast

INTRODUCTION

Bioethanol is a promising candidate as an alternative source of energy in an era of increasing fossil fuel deficit. Bioethanol is mostly used as blending agent with gasoline to cut down carbon monoxide and other smog-causing emissions. Traditional carbohydrate rich biomass from *e.g.*

corn or wheat, can be fermented to make bioethanol. However this raises a separate conflict, the conflict between food and fuel as they share the same origin (Solomon 2010). This has stimulated research for alternative methods of producing bioethanol *e.g.* via the usage of lignocellulosic biomass to produce bioethanol. Lignocellulosic plant biomass, as a by-product of agriculture and forestry, contains a considerable amount of D-xylose along with D-glucose, in a typical mass ratio of 1:2 (Carroll and Somerville 2009; Gírio *et al.* 2010). *Saccharomyces cerevisiae* can be used to make bioethanol from lignocellulosic plant biomass, however, only upon the expression of a xylose reductase and xylitol dehydrogenase (Jeffries and Jin 2004; Hahn-Hagerdal *et al.* 2007; Bera *et al.* 2011; Young *et al.* 2011) or a xylose isomerase (Kuyper *et al.* 2004; Van Maris *et al.* 2007). In this way, D-xylose consumption can be achieved. Xylose isomerase allows the interconversion between D-xylose and D-xylulose, the latter of which can be phosphorylated by the xylulose kinase Xks1, which has been overexpressed in engineered strains (Van Maris *et al.* 2007; Peng *et al.* 2011; Zha *et al.* 2014). The resulting D-xylulose-5-phosphate enters the pentose phosphate pathway (PPP) and, via glyceraldehyde-3-phosphate and fructose-6-phosphate, D-xylose catabolism is connected to glycolysis and subsequent ethanol fermentation.

Although various mutations like *e.g.* the deletion of *GRE3* (Traff *et al.* 2001; Shao *et al.* 2009; Wisselink *et al.* 2009) have improved the ethanol yield of D-xylose consumption, slow D-xylose consumption rates, especially in the presence of glucose, lead later on in fermentation to incomplete conversion of available xylose in the feedstock, thereby resulting in economically inefficient fermentations. Co-consumption of D-xylose in the D-glucose fermentation phase can shorten fermentation times and aid in the complete fermentation of xylose in the feedstock. In

an industrial setting, it is preferred that both sugars are fermented simultaneously and at high rates (von Sivers *et al.* 1994) to generate an economically feasible and robust process. A major hurdle to obtain co-consumption of D-glucose and D-xylose, is the competitive inhibition of D-glucose on D-xylose transport into the cell (Hamacher *et al.* 2002; Sedlak and Ho 2004; Saloheimo *et al.* 2007; Reider Apel *et al.* 2016). Due to these transport issues, xylose-fermenting *S. cerevisiae* strains first consume D-glucose, before D-xylose is metabolized (Hamacher *et al.* 2002). The preferred D-glucose consumption of *S. cerevisiae* is the direct result of the sugar specificities of the hexose transporters (Hxt) (Reifenberger, Boles and Ciriacy 1997; Hamacher *et al.* 2002). The hexose transporters show the highest specificity for D-glucose and their affinity for this sugar is, on average, a 100-fold higher compared to D-xylose (Kotter and Ciriacy 1993; Hamacher *et al.* 2002). This prevents efficient D-xylose transport in the presence of high(er) concentrations of D-glucose (Young *et al.* 2012). Various approaches have been used to improve D-xylose transport including the introduction of specific D-xylose transporters derived from other organisms, but, in general, the D-xylose transport rates (V_{max}) are insufficient to allow for maximal growth and rapid conversion rates (Saloheimo *et al.* 2007; Du, Li and Zhao 2010; Runquist, Hahn-Hagerdal and Radstrom 2010; Young *et al.* 2011; Wang *et al.* 2015). In recent studies D-xylose transport, in the presence of D-glucose, has improved dramatically based on the mutagenesis of endogenous Hxt transporters. This specifically concerns a conserved asparagine (at position 366, 367, 370 and 376, in Hxt11 (Shin *et al.* 2015), Hxt36 (Nijland *et al.* 2014), Hxt7 (Farwick *et al.* 2014) and Gal2 (Farwick *et al.* 2014), respectively) which, when mutated, results in a reduced D-glucose affinity with little impact or even an improved affinity for D-xylose. D-xylose, unlike D-glucose, lacks the CH2OH group at the C5 position, and

therefore still is able to bind. In a previous study (Nijland *et al.* 2014) evolutionary engineering, of a D-glucose metabolism-deficient strain (lacking all four hexokinases), was conducted in which the yeast strain was selected for improved growth on D-xylose in the presence of high and inhibitory concentrations of D-glucose. In the evolved strain, D-xylose transport was desensitized for D-glucose inhibition because of a mutation in Hxt36 of the asparagine 367 into an isoleucine or alanine. Although the required specificity gain was achieved, the maximal transport rate (V_{max}) for D-xylose was decreased compared to the parental strain. Therefore, the evolved hexokinase deletion strain (DS71054-evoB) still showed a decreased growth rate on mineral medium containing 1% D-xylose and 10% D-glucose as compared to 1% D-xylose only (Nijland *et al.* 2014).

Here, we have employed further evolutionary engineering with the goal to obtain a strain that exhibits maximal growth rates on D-xylose in the presence of D-glucose. This resulted in a set of new evolved strains that show the desired phenotype. Upon co-fermentation of the D-xylose "specialist" with a D-glucose-fermenting strain co-consumption, an improved ethanol yield was achieved.

MATERIALS AND METHODS

Yeast stains, media and culture conditions

Xylose-fermenting *S. cerevisiae* strains used in this study were provided by DSM Bio-based Products & Services and described elsewhere (Supplemental table 1). They are made available

for academic research under a Material Transfer Agreement (contact: johan.doesum-van@dsm.com). Aerobic turbidostat cultures of *S. cerevisiae* for the evolutionary engineering were grown in mineral medium (MM) supplemented with vitamin solution and trace elements (Luttik *et al.* 2000) in a 500 ml working-volume laboratory fermenter at a temperature of 30˚C and pH 4.5 (Applikon, Schiedam, the Netherlands). The dissolved oxygen (DO) set point was 20%, stirring was performed at 400 rpm and the OD_{600} was kept between 2 – 3 via CO_2 off-gas measurements. Aerobic shake flask experiments were done at 200 rpm in mineral medium supplemented with various concentrations of D-xylose and/or D-glucose. In the fermentation experiments (on 7% D-glucose and 3% D xylose or solely 7% D-glucose) a starting OD_{600} of 2.0 was used. Cell growth was monitored by optical density (OD) at 600 nm using an UV-visible spectrophotometer (Novaspec PLUS).

Analytical methods

High performance liquid chromatography (Shimadzu, Kyoto, Japan) was performed using an Aminex HPX-87H column at 65°C (Bio-RAD) and a refractive index detector (Shimadzu, Kyoto, Japan) was used to measure the concentrations of D-glucose, D-xylose, acetic acid and ethanol. The mobile phase was 0.005 N H_2SO_4 at a flow rate of 0.55 ml/min.

Transport Assays

To determine the kinetic parameters of sugar transport, cells were grown for 16 hours in shake flasks in MM containing 2% D-xylose or 2% D-glucose and standard uptake procedure was followed as shown before (Nijland *et al.* 2014). Uptakes were performed with [^{14}C] D-xylose and [^{14}C] D-glucose (ARC, USA) at 50 and 500 mmol l^{-1}, respectively, with various inhibiting sugar concentrations. The uptakes with [^{14}C] D-xylose and [^{14}C] D-glucose were performed for 60 and 10 seconds, respectively, within their linear range of uptake.

Cell volume and surface area determination

DS71054-evo6 and DS71054 were aerobically cultivated for 16 hours in minimal medium with 2% D-xylose. During the mid-exponential phase, 200 µL of each culture was harvested and centrifuged at 3000× g for 3 minutes. The supernatant was discarded and the cell pellet was resuspended in 20 µL minimal medium containing 2% D-xylose.

An aliquot of 2 µL of each resuspension was dropped on a microscope cover glass slide (22 × 40 mm), and overlaid with an agarose pad (5 × 5 mm). An amount of 0.2 gram of agarose was dissolved in 20 mL minimal medium containing 2% D-xylose by slowly heating. Molten agarose solution was solidified in a petri dish for 20 minutes in room temperature. A 5 × 5 mm agarose pad was excised with a razor blade. Bright field pictures were captured using a microscope (Nikon Ti) with the 100× objective and immersion oil. Cells in all pictures were segmented by a

plug-in BudJ v4.3 in the software ImageJ 1.48v. This plug-in draws an ellipse that best fits to each cell, returning the value of major axis (R) and minor axis (r). With these two parameters, the cell volume, surface area and surface area to volume ratio of individual cell were calculated with the following equations:

Cell volume: $V = \frac{4}{3} \times \pi \times R \times r^2$; Eq.(1)

Surface area: $S = 2 \times \pi \times r \times \left(r + R\frac{arsine}{e}\right)$; Eq.(2)

where $e = \sqrt{1 - \frac{r^2}{R^2}}$; Eq.(3)

For cell size estimation, around 100 cells were chosen for each biological replicate. To minimize bias, all mother and daughter cells within a field of view were selected. The ratio between surface area and volume was determined for each individual cell.

Ploidy analysis using flow cytometry

DS71054-evo6 and DS71054 were aerobically cultivated for 16 hours in minimal medium with 2% D-xylose. The diploid strain of CEN.PK113-7D was cultivated, as control, in the same medium complemented with 2% D-glucose. The cells were subsequently harvested, fixated, treated with RNAse and Pepsin and stained with propidium iodide using the protocol of Haase et.al. (Haase and Lew 1997). The Accuri C6 flow cytometer (BD Biosciences, CA, USA) was used in which 20 µL was injected with a FSC value > 80.000 and using the FL2 detector (585BP).

RNA extraction and cDNA synthesis

Total RNA was isolated from *S. cerevisiae* cells by a glass-bead disruption Trizol extraction procedure and performed as described by manufacturer (Life Technologies, Bleiswijk, The Netherlands). Yeast pellets from 2 ml of exponential phase cell culture (OD_{600} of ~ 4) were mixed with 0.2 ml of glass beads (diameter 0.45 mm) and 900 µl of Trizol with 125 µl chloroform, and disrupted in a Fastprep FP120 (Thermo Savant) for 45 seconds at speed 6. The extracted total RNA (500 ng) was used to synthesize cDNA using the iScript cDNA synthesis Kit (Bio-rad, CA, USA).

RNAseq and analysis

Total RNA of DS71054 and DS71054-evo6, grown in MM containing 6% D-glucose and 3% D-xylose, was isolated in duplicates after 7 hours. The RNA library was prepared for sequencing using the BGISEQ (PE100) normal DNA library construction yielding 1.6 Gb of cleaned data (BGI, Copenhagen, Denmark). The FastQ files were run through a BowTie2-TopHat-SamTools pipeline and the resulting BAM files were analysed using SeqMonk V0.27.0. The Cen.PK113-7D strain was used as a reference genome. All genes were quantified in CPM (count per million) with a cut-off of 20 and run in an intensity difference statistical test in which a statistical difference of below 0.05 was used ($p<0.05$).

Genome sequencing and analysis

Genomic DNA of DS71054, DS71054-evoB, DS71054-evo4 and DS71054-evo6 was isolated using the YeaStar ^{TM} Genomic DNA Kit (Zymo Research, Irvine, USA) and was sent to Eurofins Genomics (Ebersberg, Germany) for genomic library preparation and paired end Illumina sequencing at a read length of 2 x 150 bp. For DS71054, DS71054-evoB, DS71054-evo4 and DS71054-evo6 on average 11 million reads were analysed with a fragment size of 150 bp of which approximately 70% could be aligned to Cen.PK113-7D which was used as reference genome. The Breseq sequencing pipeline was used to detect mutations, indels and new junctions (Deatherage and Barrick 2014).

RESULTS

Evolutionary engineering

A quadruple hexokinase deletion mutant DS71054-evoB strain was previously evolved using an evolutionary engineering approach to select for growth on D-xylose in the presence of gradually increasing D-glucose concentrations (Nijland *et al.* 2014). This resulted in D-glucose-tolerant growth on D-xylose. This phenotype could be assigned to a mutation at position N367 in the endogenous chimeric Hxt36 transporter causing a defect in D-glucose transport while still allowing uptake of D-xylose. In this study, this strain was used as starting point for a new evolutionary engineering approach aiming to develop a strain that grows nearly as well on D-

xylose in the absence and presence of high D-glucose concentrations. Herein, cells were grown aerobically in a turbidostat on 1% D-xylose in the presence of 10% D-glucose. In this set-up the aerobic growth rate equals the dilution rate which on D-glucose ranges between 0.40 h^{-1} (Van Hoek, Van Dijken and Pronk 1998) and 0.49 h^{-1} (Hanscho *et al.* 2012) depending on medium composition and strain background. The growth rate on D-xylose is lower as compared to D-glucose (reviewed by Moysés et al. 2016) while the original hexokinase deletion strain DS71054 shows hardly any growth on 1% D-xylose in the presence of 10% D-glucose (Nijland *et al.* 2014). At the start of the evolutionary engineering of DS71054-evoB, the dilution rate was set at 0.14 h^{-1}, but increased gradually to 0.33 h^{-1} within a period of three months (Supplemental Figure 1). Throughout this process, samples were taken and re-streaked on mineral medium plates containing 1% D-xylose and 10% D-glucose. Single colony isolates were obtained after 31, 52, 68 and 85 days and named DS71054-evo3, DS71054-evo4, DS71054-evo5 and DS71054-evo6, respectively. The improved D-xylose growth rates of these strains in the presence of D-glucose were confirmed in shake flasks wherein DS71054 was unable to growth while the evolved strains showed gradually increased growth rates depending on the stage of the evolutionary engineering (Figure 1). DS71054-evo5, however, showed very inconsistent growth rates in MM containing 1% D-xylose and 10% D-glucose or on 1% D-xylose alone and was not used for further analysis. The other three evolved strains (DS71054-evo3, DS71054-evo4 and DS71054-evo6) showed identical growth rates on MM containing only 1% D-xylose (data not shown). The improved growth rates of DS71054-evo6 on 1% D-xylose in the presence of 10% D-glucose almost equaled the growth rates on 1% D-xylose solely (Figure 1, inset). DS71054-evo6 showed a tendency to flocculate especially on MM containing D-glucose. Dry-weight (DW) analysis

showed equal OD_{600}/mgDW ratios for the DS71054 compared to DS71054-evo6 (data not shown) to confirm that in further experiments the normalization based on OD_{600} was not affected.

Improved D-xylose uptake in evolutionary evolved strains

D-xylose uptake experiments were performed to investigate if the improved growth rates of the evolved DS71054 strains could be attributed to an elevated rate of D-xylose uptake and/or improved insensitivity of uptake towards D-glucose. D-xylose uptake rates, as measured at 50 mM concentration, were almost identical for DS71054, DS71054-evoB, DS71054-evo3 and DS71054-evo6 (15.6 ± 0.8, 15.4 ± 1.1, 13.6 ± 0.2 and 16.0 ± 1.3 nmol/mgDW.min, respectively) (Figure 2). Next, the sensitivity of D-xylose uptake to D-glucose was analyzed with 50 mM D-xylose and increasing D-glucose concentrations. Now, the DS71054-evo6 strain showed significant improved D-xylose uptake in the presence of high concentrations of D-glucose as compared to DS71054-evoB and DS71054-evo3 (Figure 2) and these data correlate with the improved growth rates on D-xylose in the presence of high concentrations of D-glucose (Figure 1). D-glucose uptake, at a saturating concentration of 500 mM, by DS71054 and the evolved mutant strains evo3-evo6 showed no clear trend but was not decreased during the evolution (Supplemental Figure 2). To identify the possible targets responsible for the glucose tolerant D-xylose uptake, all highly expressed *HXT* transporters (*HXT1-7*) of DS71054-evo3, DS71054-evo4 and DS71054-evo6 were sequenced. In none of these Hxt transporters mutations were identified, but amplification of *HXT7* failed in DS71054-evo6. Further analysis revealed that in

DS71054-evo6 *HXT36* was fused to *HXT7* at position 1209 creating a novel chimer *HXT37*, explaining also the failed amplification of *HXT7* in DS71054-evo6. The rearrangements from *HXT3* to *HXT36* and to *HXT37* are most likely based on a fragment of 240 bp which is entirely conserved in all three transporters. *HXT37* differs from *HXT36* at 3 base-pairs (T1623C, G1657A and T1668C) of which only one causes an amino acid change (A556T). The isoleucine mutation at position 367, responsible for the decreased D-glucose affinity in Hxt36, however, remained unaltered (Figure 3).

In order to determine if Hxt37 N367I is responsible for the improved D-xylose uptake in DS71054-evo6, uptake experiments were performed using the hexose transporter deletion strain DS68625 overexpressing Hxt36 N367I (Nijland *et al.* 2014) and Hxt37 N367I. In both strains D-xylose uptake was measured in the presence of various concentrations of D-glucose, but no differences in uptake characteristics were observed between both chimeras (Supplemental Figure 3). Likewise, no difference in the D-xylose affinity and transport rate between both chimeric transporters was evident (Supplemental Figure 4).

Morphological analysis and ploidy analysis

In order to study possible morphological changes in DS71054-evo6 compared to DS71054, both strains were aerobically cultivated in MM containing 2% D-xylose for 16 hours. The average cell volume and cell surface was measured using ImageJ and BudJ. The cell surface area (Figure 4) of DS71054-evo6 (92.3 ± 3.5 μm^2) was significantly enlarged as compared to DS71054 (61.3 ± 2.3 μm^2) which increased the cell volume almost 2-fold; from 45.6 ± 2.6 μm^3 to 82.2 ± 5.5 μm^3 in

DS71054 and DS71054-evo6, respectively (Figure 4, Supplemental Figure 5). The increased cell surface area was not observed in the other evolved predecessors (data not shown), whereas these also show improved D-xylose uptake, albeit to a lesser extent. Therefore, the increased cell surface is only one of the factors in the improved D-xylose phenotype in DS71054-evo6.

Increased cell volume, due to increased ploidy, was observed in previous studies using evolutionary engineering (Oud *et al.* 2013; Venkataram *et al.* 2016; Papapetridis *et al.* 2018). In order to analyze the ploidy of DS71054-evo6 the strain was subjected to propidium iodide staining of the DNA content (Haase and Lew 1997). The haploid DS71054 strain and the diploid CEN.PK113-7D strain were used as controls. Flow cytometry analysis using FACS yielded a single and double (of dividing cells) copy of the genome in DS71054 strain and double and quadruple (of dividing cells) copies in the diploid CEN.PK113-7D strain. The DS71054-evo6 genomic copy number clearly coincides with the diploid CEN.PK113-7D strain therefor we conclude that the cell size increase is due to genome duplication from haploid to diploid (Supplemental Figure 6).

Transcriptomic analysis

Transcriptional analysis was performed in DS71054 and the evolved strain DS71054-evo6. In order to keep the growth rates comparable, the strains were grown aerobically in MM containing 3% D-xylose, in the presence of 6% D-glucose, for 7 hours. The total mRNA was isolated and sequenced in duplicate and the fold changes (FC) were determined comparing the DS71054 strain with DS71054-evo6. In comparison, 88 genes were at least 3-fold up-regulated (Supplemental Table 2) and 113 genes were at least 3-fold down-regulated (Supplemental Table

3) in DS71054-evo6 as compared to the DS71054 strain. Flo1, a lectin-like protein involved in flocculation, shows a major up-regulation (55.5x FC) explaining the flocculating phenotype. In the genome database of CEN.PK113-7D, the predecessor of the DS71054 lineage, Flo1 is missing (Nijkamp *et al.* 2012). A similar observation was made in a recent study (Jenjaroenpun *et al.* 2018) but here *FLO1* was annotated as A0096W, which is located on chromosome 1 and which shows about 80 and 81 % identity with Flo1 at the DNA and protein level, respectively. Upon deletion of *FLO1* (or A0096W) in the DS71054-evo6 strain, the flocculation was abolished (data not shown). However, the phenotype of increased cell size of DS71054-evo6-Δflo1 and the improved D-xylose consumption in the presence of D-glucose was not altered (data not shown).

Importantly, in the DS71054-evo6 strain, the transporters genes of the *HXT* family show a remarkable down-regulation: *HXT1* (8.8-fold), *HXT2* (17.1-fold), *HXT5* (4.2-fold) and *HXT7* (∞). The apparent down-regulation of *HXT7* in DS71054-evo6 is due to the formation of the chimeric Hxt37. On the other hand, expression of the Hxt36/Hxt37 N367I mutant is not significantly altered in DS71054-evo6 as compared to the DS71054 strain. Overall, the Hxt transporter landscape in DS71054-evo6, is severely altered leaving only two highly expressed Hxt transporters in DS71054-evo6, *i.e.* Hxt37 N367I and Hxt4 (Figure 5). Furthermore, the expression of all plasma membrane transporters combined, which is mainly based on the severe down-regulation of the hexose transporters, is decreased by 21 ± 0.1 % in DS71054-evo6 compared to DS71054. In contrast, the combined expression levels of all genes is decreased by only 1 ± 0.04 %. The decreased expression of transporters could create additional space on the cytoplasmic membrane for an enhanced expression of Hxt37-N367I. Space limitations for permease insertion in the cytoplasmic membrane was observed earlier (Hennaut, Hilger and

Grenson 1970). These results suggest that the improved D-xylose consumption by the evolved DS71054-evo6 strain is also caused by the reduced expression of *HXT1*, *HXT2* and *HXT5* and the deletion of *HXT7*.

Among the up-regulated genes three distinct groups were detected (using the String-database; https://string-db.org/): cell cycle progression (*e.g. CLB1*, *CLN2* and *SWI5*), methionine metabolism (*e.g. MET1*, *MET3* and *MET5*) and iron/copper metabolism (*e.g. TIS1*, *FET3* and *CCC2*). The genes involved in cell cycle progression are most likely upregulated due to the change in ploidy in DS71054-evo6. Upregulation observed for: Clb2 (8.2 ± 0.5), Pcl1 (5.7 ± 0.8), Clb1 (4.5 ± 0.3), Cln2 (4.1 ± 0.3), Swi5 (3.9 ± 0.2) and Cln1 (3.8 ± 0.2). To our knowledge, there is no relationship between methionine metabolism or iron/copper metabolism and xylose transport/consumption.

Genome Analysis

To further identify the genotypic changes in the evolved strains, genome sequencing was performed. This revealed 50 coding mutations in the DS71054 strain as compared to CEN.PK113-7D (Nijkamp *et al.* 2012) of which 36 cause an amino acid change. DS71054 was used as a new reference to analyze the mutations in DS71054-evoB, DS71054-evo4 and DS71054-evo6. In DS71054-evoB, the N367I mutation was first introduced and remained unaltered in DS71054-evo4 and DS71054-evo6. Some mutations in DS71054-evo4 were lost in DS71054-evo6 and were therefore considered as not relevant for the altered phenotype. The S317Y mutation in Mal11, encoding a high-affinity maltose transporter, seems interesting in

relation to a recent report suggesting that Mal11, when overexpressed, improves growth on D-xylose (Guirimand *et al.* 2019). Importantly, in that study a direct role of Mal11 in D-xylose uptake was not confirmed. To test if the S317Y mutation could change the specificity of Mal11 towards D-xylose, Mal11 and Mal11 S317Y were overexpressed in strain DS68625 (Nijland *et al.* 2014). Both transporters were unable to restore growth on D-xylose unlike overexpression of Hxt2 (Supplemental Figure 7A). In contrast, Mal11 supported growth on D-glucose by strain DS68625. Interestingly, the Mal11 S317Y mutant was unable to support growth on D-glucose (Supplemental Figure 7B) suggesting that the mutation caused a further decrease in D-glucose uptake capacity of the DS71054-evo6 strain. A further interesting mutation (G369S) in DS71054-evo4 (Table 1) was observed in Pbs2 which encodes a Mitogen-Activated Protein Kinase Kinase (MAPKK), an scaffold protein integral to the osmoregulatory HOG (High-osmolarity glycerol) signaling pathway which affects gene expression (Hohmann 2009). Deletion of Hog1, as well as Pbs2, severely decreased the Hxt1 expression level (Tomás-Cobos *et al.* 2004) which could link the G369S mutation in Pbs2 to reduced expression of Hxt1 in DS71054-evo4. Furthermore, Pbs2 in DS71054-evo6 obtained another mutation ($Q60^{stop}$) causing a truncation of Pbs2 therefore significantly lowering the expression level of Hxt1. The other mutations observed in DS71054-evo4 and DS71054-evo6 could contribute to the phenotype as well but no direct evidence was found that these genes influence the expression of the hexose transporter landscape or glycolysis (Table 1). Notably, all observed mutations and SNPs were homozygous in DS71054-evo6 indicating that the change in ploidy in this strain occurred in the last phase of the evolutionary engineering.

Mixed culture fermentations

To examine co-consumption of D-glucose and D-xylose, a mixed strain fermentation, including the D-glucose consuming strain CEN.PK113-7D and the improved D-xylose consuming strain DS71054-evo6-Δflo1, was compared to the DS68616 strain which consumes D-glucose and D-xylose sequentially. The DS68616 strain was chosen for comparison with the two strain set-up since it is an industrially developed strain, and therefore consumes D-xylose fast. Industrial sugar concentrations were used of 7 % D-glucose and 3 % D-xylose and the DS68616 strain was inoculated at a starting OD_{600} of 10 whereas the mixture of DS71054-evo6-Δflo1 and CEN.PK113-7D was inoculated in a 2:1 ratio at a starting OD_{600} of 6.67 and 3.33, respectively (Figure 6). During the fermentation the strain ratio was analyzed using qPCR in which the *GRE3* gene was amplified of Cen.PK113-7D and a fragment spanning the promotor region and the terminator region outside of the deleted *GLK1* gene of DS71054-evo6-Δflo1. *ACT1* was used as reference to normalize for the amount of DNA (Supplemental Table 4). This ratio changed from 2:1 to 1:2, which fits the theoretical ratio based on sugar consumption (Supplemental Figure 8). In the single strain fermentation the D-xylose conversion rate (Q D-xylose) in the DS68616 strain is, due to the inhibiting effect of D-glucose on D-xylose transport, low (0.128 ± 0.007 g D-xylose/gDW.h) in the first 10 hours of the fermentation and increases only upon the (complete) consumption of D-glucose. In the mixed strain fermentation, D-xylose consumption starts immediately at increased D-xylose conversion rate (0.330 ± 0.007 g D-xylose/gDW.h) even with the decreased cell density (OD_{600}) of 6.67 of DS71054-evo6-Δflo1 as compared to DS68616 (OD_{600} of 10). The gDW (gram dry weight) normalization in the mixed strain fermentation was

performed using the combined OD_{600} of CEN.PK113-7D and DS71054-evo6-Δflo1. The D-glucose conversion rate, due to the lower inoculum of CEN.PK113-7D, is decreased to 0.661 ± 0.015 g D-glucose/gDW.h versus 0.877 ± 0.041 g D-glucose/gDW.h in DS68616. The improved co-consumption of DS71054-evo6-Δflo1 and CEN.PK113-7D yields, at the end of the fermentation (15 hours), significantly decreased residual sugar concentrations of 4.58 ± 0.07 g sugar as compared to DS68616 (8.76 ± 1.0 g sugar) (Table 2). Furthermore, the DS71054-evo6-Δflo1 and CEN.PK113-7D mixture showed a decreased yield (Y) of glycerol (0.045 ± 0.001 g glycerol/g sugar) and biomass (0.0866 ± 0.0034 gDW/g sugar) but increased production yield of ethanol (0.386 ± 0.004 g ethanol/g sugar) (Table 2).

DISCUSSION

The use of lignocellulosic biomass for ethanol production is a promising technology for the additional supply of energy from renewable and non-food resources. The main hurdle to overcome is the efficient co-fermentation of hexoses and pentoses since transport rates for pentoses in general, and D-xylose in particular, are insufficient. In recent studies, strains lacking all hexokinases have been used to improve the D-xylose specificity of the endogenous hexose transporters, and most significant results were obtained by mutation of a conserved asparagine in transmembrane segment 8 in a set of Hxt transporters (Farwick *et al.* 2014; Nijland *et al.* 2014; Reznicek *et al.* 2015; Shin *et al.* 2015). This mutation reduces or even abolishes D-glucose transport, while having little impact on the D-xylose transport affinity. However, a major caveat with the mutation is that it reduces the D-xylose transport rate, whereas high rates are required

for efficient D-xylose utilization. To elevate glucose-insensitive rates of D-xylose uptake, we have conduced further evolutionary engineering of the hexokinase deletion strain DS71054-evoB that contains the N367I mutation in the chimeric Hxt36 transporter (Nijland *et al.* 2014). More stringent conditions were imposed to allow these cells to grow with high rates on D-xylose in the presence of competing D-glucose and this yielded the DS71054-evo6 strain which shows a growth rate on D-xylose in the presence of a 10-fold concentration of D-glucose which is nearly identical to the growth rate on solely D-xylose. Transcriptome and genomic analysis demonstrate that in this strain the transporter landscape has been altered quite dramatically. First, Hxt36 N367I was converted into Hxt37 N367I. Although the uptake characteristics remained unchanged, the Hxt37 N367I fusions resulted in the loss of the D-glucose transporter Hxt7. Possibly, this fusion also leads to a more stable localization in the plasma membrane of the Hxt37 protein making it less sensitive glucose-induced downregulation (catabolite inactivation). Due to mutations in Pbs2 in DS71054-evo4 and DS71054-evo6, the expression of Hxt1 is severely decreased. In DS71054-evo6, also Hxt2 showed significantly reduced expression levels, leaving Hxt4 as the only D-glucose transporter. In these strains, D-glucose uptake is further decreased by the S317Y mutation in the maltose transporter Mal11 which can support glucose uptake when overexpressed. Importantly, the down-regulation and deletion of the Hxt transporters could lead to an increase in “plasma membrane space” thereby possibly allowing improved localization and/or decreased D-glucose-induced proteolytic degradation (Krampe *et al.* 1998) of Hxt37 N367I. This may contribute to overall reduced sensitivity of D-xylose uptake for D-glucose. Interestingly, uptake rate of several exogenous substrates have been measured in a series of isogenic *S. cerevisiae* strains that were haploid, diploid, triploid and tetraploid

(Hennaut, Hilger and Grenson 1970). For three substrates, whose transport is catalyzed by constitutively expressed permeases, the relative uptake rate (in unit of cell mass or in unit per genome) was decreased in the same proportions as the surface to volume ratio. For other substrates, whose transport is inducible, this limitation was not observed. It was suggested that the space for permease insertion in the cytoplasmic membrane is limited for the constitutive permeases studied (Hennaut, Hilger and Grenson 1970). In this respect, we previously observed that upon the expression of Hxt11-GFP in the Hxt deletion strain (DS68625) and parental DS68616 strain, a higher level of GFP localized to the cytoplasmic membrane in the DS68625 Hxt deletion strain (Shin HY, personal communications).

Not only the overall expression of Hxt transporter genes was decreased, also the cell surface area of the DS71054-evo6 strain as compared to DS71054 was significantly enlarged. Cell volume in *S. cerevisiae* is related to ploidy and indeed flow cytometric analysis showed diploidy in DS71054-evo6 whereas the DS71054 strain, as the starting point of the evolutionary engineering, was haploid. The increased cell surface area, caused by the genome duplication, may also contribute to an improved expression of the specific D-xylose transporter Hxt37 N367I. Although changes in ploidy has been studied extensively, the exact advantage of diploid strains, excluding the increased resistance towards harmful mutations (Janssen *et al.* 2011; Crasta *et al.* 2012), is still unclear (Gorter de Vries, Pronk and Daran 2017). In industrial settings, in which *S. cerevisiae* grows under stress conditions, increased genome copy numbers have been observed (reviewed by Gorter de Vries, Pronk and Daran 2017).

In a mixed strain fermentation with a D-glucose specialist (CEN.PK113-7D) and a D-xylose specialist (DS71054-evo6-Δflo1) co-consumption of both sugars was observed with decreased

residual sugar concentrations at the end of the fermentation. Decreased biomass and glycerol yield allowed for increased ethanol yield in the mixed strain fermentation (0.386 ± 0.004 g/g sugar) versus DS68616 (0.372 ± 0.0007 g/g sugar). A similar mixed strain fermentation was shown recently with three strains consuming D-glucose, D-xylose or L-arabinose (Verhoeven *et al.* 2018). However, D-xylose consumption was still severely inhibited, most likely because D-xylose uptake was insufficient.

CONCLUSIONS

Evolutionary engineering is an effective method to improve D-xylose consumption in the presence of high concentrations of D-glucose by a D-xylose consuming *S. cerevisiae* strain in which the four hexokinase genes are deleted. The evolved strain supports high rates of D-xylose fermentation at industrial relevant sugar concentrations, which is accompanied with an altered morphology (due to the genome duplication) and a changed transporter landscape. Glucose insensitive D-xylose transport, via a novel chimeric Hxt37 transporter and the down-regulation of many Hxt transporters in the evolved strain resulted in an elevated rate of glucose-insensitive D-xylose consumption. Co-fermentation of the improved D-xylose fermenting strain together with a D-glucose consuming strain improved the fermentation rate and ethanol yield at industrial relevant carbohydrate concentrations

Acknowledgements

This work was performed within the BE-Basic R&D Program (http://www.be-basic.org), which is financially supported by the Dutch Ministry of Economic Affairs, Agriculture and Innovation (EL&I). DSM co-funded the research described in this publication in the framework of BE-Basic. We thank Matthias Heinemann for discussions.

Conflict of Interest

PW works for DSM. DSM markets technology for biofuels production from lignocellulosic feedstocks, holds IP positions in this field.

List of abbreviations: bp: base pair; DW: dry-weight; FC: fold change; Hxt: hexose transporter; MM: mineral medium; OD: optical density; XKS: xylulose kinase; XI: xylose isomerase.

Author contributions: JN**,** HS, PW and AD conceived and designed the research; JN and XL performed the experiments; PW constructed strains; AD supervised the project; the manuscript was written by the contributions of JN and AD, and corrected by all authors.

REFERENCES

Bera AK, Ho NWY, Khan A *et al.* A genetic overhaul of Saccharomyces cerevisiae 424A(LNH-ST) to improve xylose fermentation. *J Ind Microbiol Biotechnol* 2011;**38**:617–26.

Carroll A, Somerville C. Cellulosic biofuels. *Annu Rev Plant Biol* 2009;**60**:165–82.

Crasta K, Ganem NJ, Dagher R *et al.* DNA breaks and chromosome pulverization from errors in

mitosis. *Nature* 2012;**482**:53–8.

Deatherage DE, Barrick JE. Identification of mutations in laboratory-evolved microbes from next-generation sequencing data using breseq. *Methods Mol Biol* 2014;**1151**:165–88.

Du J, Li S, Zhao H. Discovery and characterization of novel d-xylose-specific transporters from Neurospora crassa and Pichia stipitis. *Mol Biosyst* 2010;**6**:2150–6.

Farwick A, Bruder S, Schadeweg V *et al.* Engineering of yeast hexose transporters to transport D-xylose without inhibition by D-glucose. *Proc Natl Acad Sci* 2014:1323464111-.

Gírio FM, Fonseca C, Carvalheiro F *et al.* Hemicelluloses for fuel ethanol: A review. *Bioresour Technol* 2010;**101**:4775–800.

Gorter de Vries AR, Pronk JT, Daran JMG. Industrial relevance of chromosomal copy number variation in Saccharomyces yeasts. *Appl Environ Microbiol* 2017;**83**, DOI: 10.1128/AEM.03206-16.

Guirimand GGY, Bamba T, Matsuda M *et al.* Combined cell surface display of β-D-glucosidase (BGL), maltose transporter (MAL11) and overexpression of cytosolic xylose reductase (XR) in *Saccharomyces cerevisiae* enhance cellobiose/xylose co-utilization for xylitol bio-production from lignocellulosic biomass. *Biotechnol J* 2019:1800704.

Haase SB, Lew DJ. Flow cytometric analysis of DNA content in budding yeast. *Methods Enzymol* 1997;**283**:322–32.

Hahn-H?gerdal B, Karhumaa K, Jeppsson M *et al.* Metabolic Engineering for Pentose Utilization

in Saccharomyces cerevisiae. *Biofuels*. Vol 108. Berlin, Heidelberg: Springer Berlin Heidelberg, 2007, 147–77.

Hamacher T, Becker J, Gardonyi M *et al.* Characterization of the xylose-transporting properties of yeast hexose transporters and their influence on xylose utilization. *Microbiology* 2002;**148**:2783–8.

Hanscho M, Ruckerbauer DE, Chauhan N *et al.* Nutritional requirements of the BY series of *Saccharomyces cerevisiae* strains for optimum growth. *FEMS Yeast Res* 2012;**12**:796–808.

Hennaut C, Hilger F, Grenson M. Space limitation for permease insertion in the cytoplasmic membrane of Saccharomyces cerevisiae. *Biochem Biophys Res Commun* 1970;**39**:666–71.

Van Hoek P, Van Dijken JP, Pronk JT. Effect of specific growth rate on fermentative capacity of baker's yeast. *Appl Environ Microbiol* 1998;**64**:4226–33.

Hohmann S. Control of high osmolarity signalling in the yeast *Saccharomyces cerevisiae*. *FEBS Lett* 2009;**583**:4025–9.

Janssen A, Van Der Burg M, Szuhai K *et al.* Chromosome segregation errors as a cause of DNA damage and structural chromosome aberrations. *Science (80-)* 2011;**333**:1895–8.

Jeffries TW, Jin YS. Metabolic engineering for improved fermentation of pentoses by yeasts. *Appl Microbiol Biotechnol* 2004;**63**:495–509.

Jenjaroenpun P, Wongsurawat T, Pereira R *et al.* Complete genomic and transcriptional landscape analysis using third-generation sequencing: a case study of Saccharomyces

cerevisiae CEN.PK113-7D. *Nucleic Acids Res* 2018, DOI: 10.1093/nar/gky014.

Kotter P, Ciriacy M. Xylose fermentation by Saccharomyces cerevisiae. *Appl Microbiol Biotechnol* 1993;**38**:776–83.

Krampe S, Stamm O, Hollenberg CP *et al.* Catabolite inactivation of the high-affinity hexose transporters Hxt6 and Hxt7 of Saccharomyces cerevisiae occurs in the vacuole after internalization by endocytosis. *FEBS Lett* 1998;**441**:343–7.

Kuyper M, Winkler AA, van Dijken JP *et al.* Minimal metabolic engineering of Saccharomyces cerevisiae for efficient anaerobic xylose fermentation: a proof of principle. *FEMS Yeast Res* 2004;**4**:655–64.

Luttik MA, Kötter P, Salomons FA *et al.* The Saccharomyces cerevisiae ICL2 gene encodes a mitochondrial 2-methylisocitrate lyase involved in propionyl-coenzyme A metabolism. *J Bacteriol* 2000;**182**:7007–13.

Van Maris AJA, Winkler AA, Kuyper M *et al.* Development of efficient xylose fermentation in Saccharomyces cerevisiae: xylose isomerase as a key component. *Adv Biochem Eng* 2007;**108**:179–204.

Moysés D, Reis V, Almeida J *et al.* Xylose Fermentation by Saccharomyces cerevisiae: Challenges and Prospects. *Int J Mol Sci* 2016;**17**:207.

Nijkamp JF, van den Broek M, Datema E *et al.* De novo sequencing, assembly and analysis of the genome of the laboratory strain Saccharomyces cerevisiae CEN.PK113-7D, a model for modern industrial biotechnology. *Microb Cell Fact* 2012;**11**:36.

Nijland JG, Shin HY, de Jong RM *et al.* Engineering of an endogenous hexose transporter into a specific D-xylose transporter facilitates glucose-xylose co-consumption in Saccharomyces cerevisiae. *Biotechnol Biofuels* 2014;**7**:168.

Oud B, Guadalupe-Medina V, Nijkamp JF *et al.* Genome duplication and mutations in ACE2 cause multicellular, fast-sedimenting phenotypes in evolved Saccharomyces cerevisiae. *Proc Natl Acad Sci U S A* 2013;**110**, DOI: 10.1073/pnas.1305949110.

Papapetridis I, Goudriaan M, Vázquez Vitali M *et al.* Optimizing anaerobic growth rate and fermentation kinetics in Saccharomyces cerevisiae strains expressing Calvin-cycle enzymes for improved ethanol yield. *Biotechnol Biofuels* 2018;**11**:17.

Peng B, Chen X, Shen Y *et al.* [Effect of controlled overexpression of xylulokinase by different promoters on xylose metabolism in Saccharomyces cerevisiae]. *Wei Sheng Wu Xue Bao* 2011;**51**:914–22.

Reider Apel A, Ouellet M, Szmidt-Middleton H *et al.* Evolved hexose transporter enhances xylose uptake and glucose/xylose co-utilization in Saccharomyces cerevisiae. *Sci Rep* 2016;**6**:19512.

Reifenberger E, Boles E, Ciriacy M. Kinetic characterization of individual hexose transporters of Saccharomyces cerevisiae and their relation to the triggering mechanisms of glucose repression. *Eur J Biochem* 1997;**245**:324–33.

Reznicek O, Facey SJ, de Waal PP *et al.* Improved xylose uptake in Saccharomyces cerevisiae due to directed evolution of galactose permease Gal2 for sugar co-consumption. *J Appl*

Microbiol 2015;**119**:99–111.

Runquist D, Hahn-Hagerdal B, Radstrom P. Comparison of heterologous xylose transporters in recombinant Saccharomyces cerevisiae. *Biotechnol Biofuels* 2010;**3**:5.

Saloheimo A, Rauta J, Stasyk O V *et al.* Xylose transport studies with xylose-utilizing Saccharomyces cerevisiae strains expressing heterologous and homologous permeases. *Appl Microbiol Biotechnol* 2007;**74**:1041–52.

Sedlak M, Ho NWY. Characterization of the effectiveness of hexose transporters for transporting xylose during glucose and xylose co-fermentation by a recombinantSaccharomyces yeast. *Yeast* 2004;**21**:671–84.

Shao Z, Zhao H, Zhao H *et al.* DNA assembler, an in vivo genetic method for rapid construction of biochemical pathways. *Nucleic Acids Res* 2009;**37**:e16–e16.

Shin HY, Nijland JG, de Waal PP *et al.* An engineered cryptic Hxt11 sugar transporter facilitates glucose–xylose co-consumption in Saccharomyces cerevisiae. *Biotechnol Biofuels* 2015;**8**:176.

von Sivers M, Zacchi G, Olsson L *et al.* Cost analysis of ethanol production from willow using recombinant Escherichia coli. *Biotechnol Prog* 1994;**10**:555–60.

Solomon BD. Biofuels and sustainability. *Ann N Y Acad Sci* 2010;**1185**:119–34.

Tomás-Cobos L, Casadomé L, Mas G *et al.* Expression of the HXT1 low affinity glucose transporter requires the coordinated activities of the HOG and glucose signalling pathways.

J Biol Chem 2004;**279**:22010–9.

Traff KL, Otero Cordero RR, van Zyl WH *et al.* Deletion of the GRE3 Aldose Reductase Gene and Its Influence on Xylose Metabolism in Recombinant Strains of Saccharomyces cerevisiae Expressing the xylA and XKS1 Genes. *Appl Environ Microbiol* 2001;**67**:5668–74.

Venkataram S, Dunn B, Li Y *et al.* Development of a Comprehensive Genotype-to-Fitness Map of Adaptation-Driving Mutations in Yeast. *Cell* 2016;**166**:1585-1596.e22.

Verhoeven MD, de Valk SC, Daran J-MG *et al.* Fermentation of glucose-xylose-arabinose mixtures by a synthetic consortium of single-sugar-fermenting Saccharomyces cerevisiae strains. *FEMS Yeast Res* 2018;**18**, DOI: 10.1093/femsyr/foy075.

Wang C, Bao X, Li Y *et al.* Cloning and characterization of heterologous transporters in Saccharomyces cerevisiae and identification of important amino acids for xylose utilization. *Metab Eng* 2015;**30**:79–88.

Wisselink HW, Toirkens MJ, Wu Q *et al.* Novel evolutionary engineering approach for accelerated utilization of glucose, xylose, and arabinose mixtures by engineered Saccharomyces cerevisiae strains. *Appl Environ Microbiol* 2009;**75**:907–14.

Young E, Poucher A, Comer A *et al.* Functional survey for heterologous sugar transport proteins, using Saccharomyces cerevisiae as a host. *Appl Environ Microbiol* 2011;**77**:3311–9.

Young EM, Comer AD, Huang H *et al.* A molecular transporter engineering approach to improving xylose catabolism in Saccharomyces cerevisiae. *Metab Eng* 2012;**14**:401–11.

Zha J, Shen M, Hu M *et al.* Enhanced expression of genes involved in initial xylose metabolism and the oxidative pentose phosphate pathway in the improved xylose-utilizing Saccharomyces cerevisiae through evolutionary engineering. *J Ind Microbiol Biotechnol* 2014;**41**:27–39.

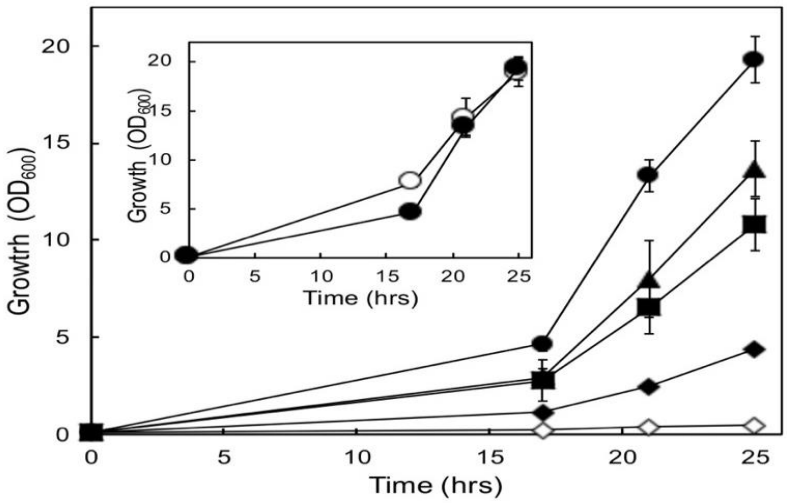

Figure 1. Growth (OD_{600}) of the DS71054 hexokinase deletion strain (◇) and the evolved derivatives DS71054-evoB (◆), DS71054-evo3 (■), DS71054-evo4 (▲) and DS71054-evo6 (●) in mineral medium supplemented with 1 % D-xylose and 10 % D-glucose. Inset shows the growth (OD_{600}) of DS71054-evo6 on 1 % D-xylose and 10 % D-glucose (●) and solely 1 % D-xylose (○). Error bars were obtained from biological triplicates.

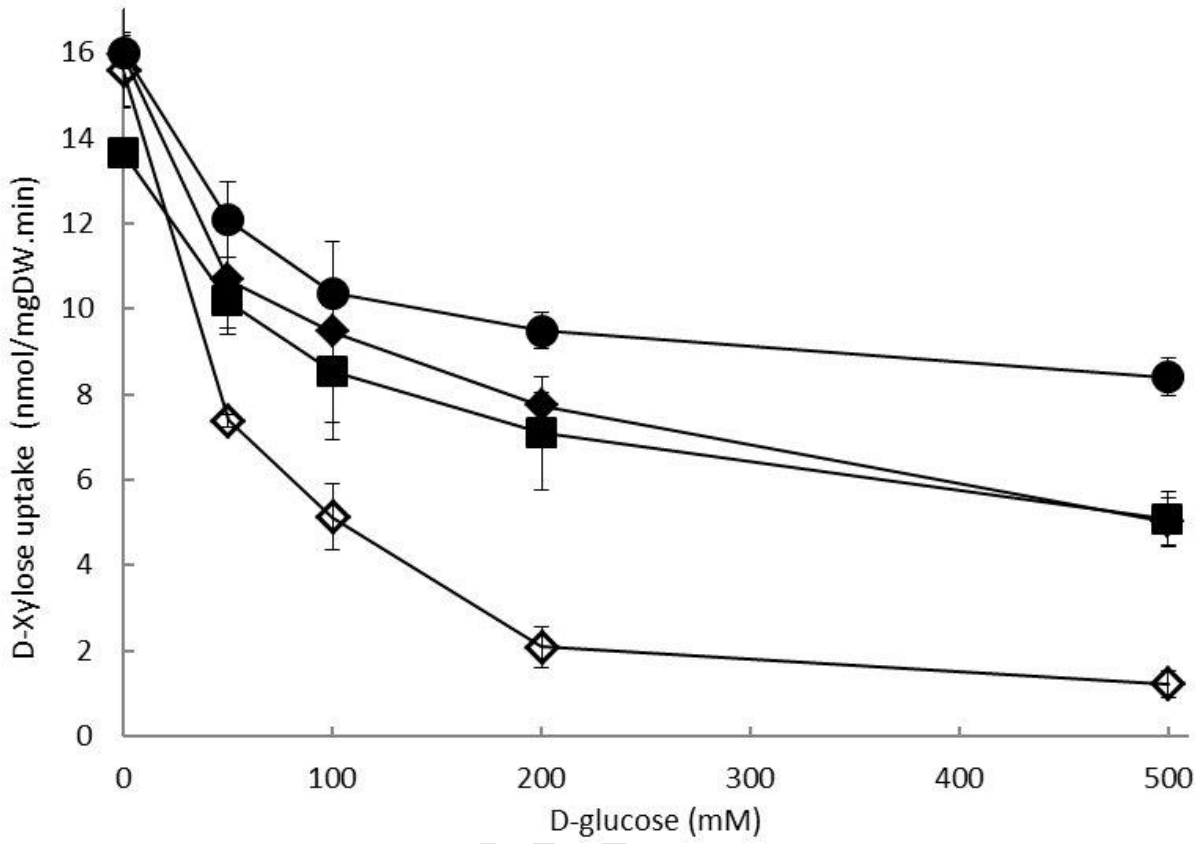

Figure 2. D-xylose uptake in DS71054 (◇), DS71054-evoB (◆), DS71054-evo3 (■) and DS71054-evo6 (●). Uptakes (in nmol/mgDW.min) were performed with 50 mM ^{14}C D-xylose and various concentrations of D-glucose (0, 50, 100, 200 and 500 mM). Errors are the standard deviation of two independent experiments.

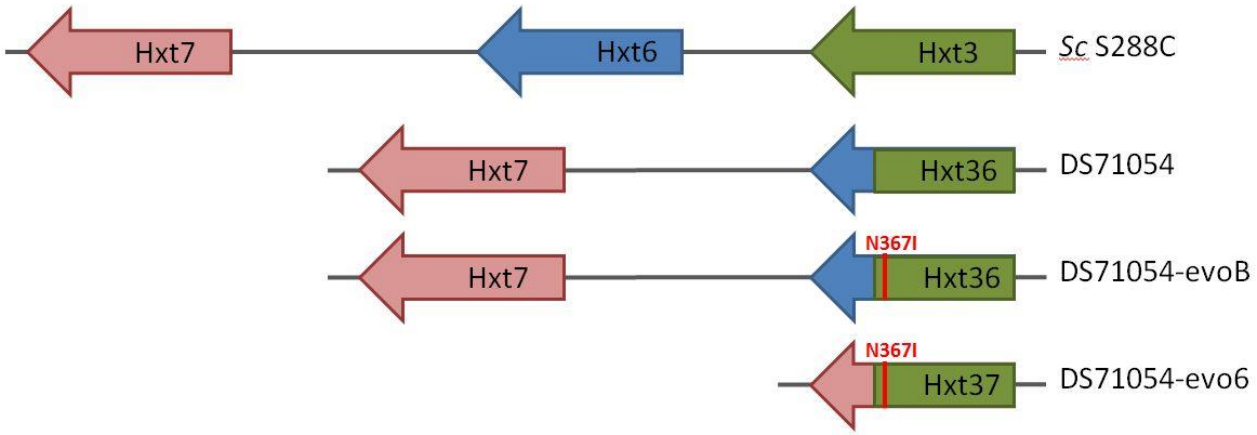

Figure 3. Genomic localization on chromosome IV of *HXT3*, *HXT6* and *HXT7* in *S. cerevisiae* S288C and the rearrangements in DS71054, DS71054-evoB and DS71054-evo6 including (in red) the asparagine to isoleucine mutation at position 367.

A

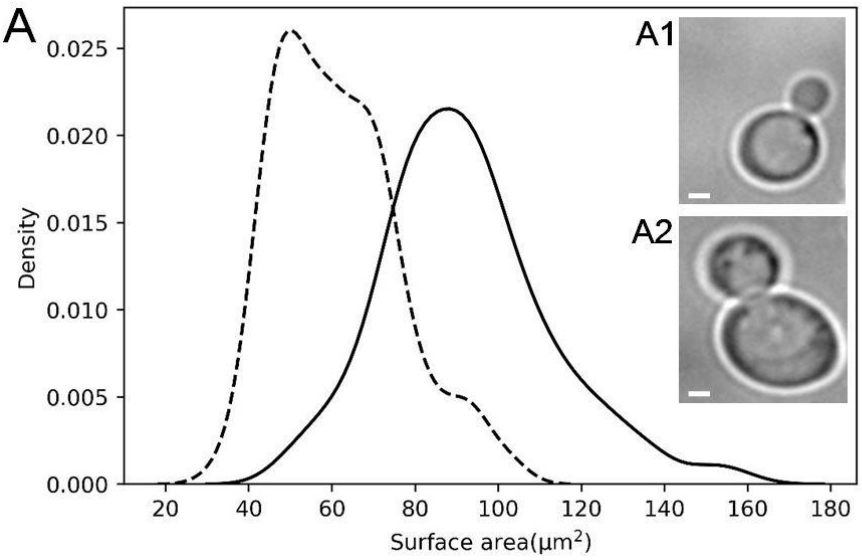

B

Strain	Volume (μm³)	Surface area (μm²)	SA/V ratio (μm⁻¹)
DS71054	45.6 ± 2.6	61.3 ± 2.3	1.40 ± 0.03
DS71054-Evo6	82.2 ± 5.5	92.3 ± 3.5	1.17 ± 0.02

Figure 4. Morphological analysis of DS71054 (A1) and DS71054-evo6 (A2) grown for 16 hours in MM containing 2% D-xylose (the white bars indicates 1 μm). The cell surface area (in μm^2) of DS71054 (dashed line) was compared to DS71054-evo6 (black line) (A). The extracted cell surface areas (in μm^2), volumes (in μm^3) and cell surface area to volume ratios (in μm) are depicted in the table (B).

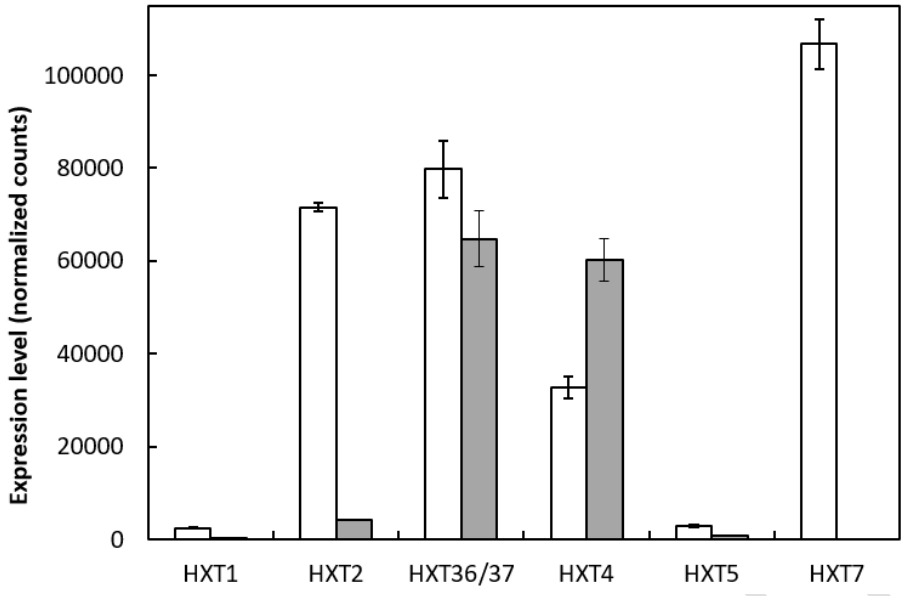

Figure 5. RNAseq data of the main Hxt transporters in the DS71054 hexokinase deletion strain (white bars) and evolved derivative DS71054-evo6 (grey bars). Depicted on the left vertical ax is the absolute normalized expression of *HXT1*, *HXT2*, *HXT36/HXT37*, *HXT4*, *HXT5* and *HXT7*. RNA was isolated after 7 hours of aerobic growth in mineral medium supplemented with 3 % D-xylose and 6 % D-glucose.

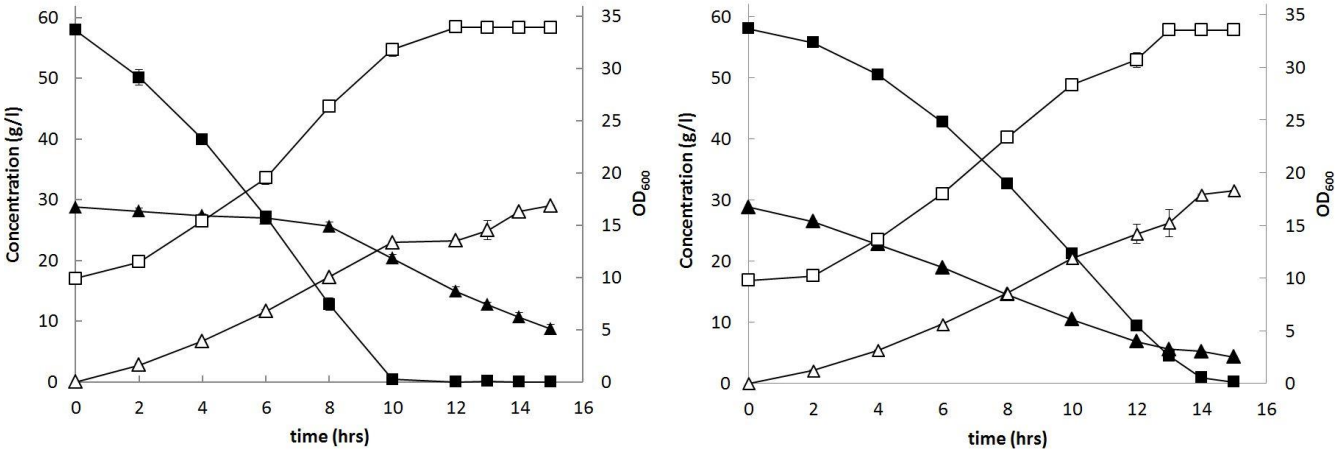

Figure 6. Anaerobic fermentation of DS68616 (A) and the mixed co-fermentation of CEN.PK113-7D together with the hexokinase deletion strain DS71054-evo6 (B) on mineral medium supplemented with 7 % D-glucose (■) and D-xylose (▲) concentration and the biomass (□) and ethanol (△) formation. Starting OD_{600} was 10.0 and the error bars were obtained from biological duplicates.

DS71054-evoB

Gene	mutation	annotation
HXT36	N367I	Low affinity glucose transporter
PHO12	Q354K	acid phosphatases

DS71054-evo4

Gene	mutation	annotation
HXT36	**N367I**	**Low affinity glucose transporter**
SPC3	V42A	Subunit of signal peptidase complex
PBS2	G369S	MAP kinase kinase of the HOG signaling pathway
URA2	F1447L	Bifunctional carbamoylphosphate synthetase
WSC4	T229I	Endoplasmic reticulum (ER) membrane protein
SUP35	Q70L	Translation termination factor eRF3; mRNA deadenylation

DS71054-evo6

Gene	mutation	annotation
Hxt37	**N367I**	**Low affinity glucose transporter**
SPC3	V42A	Subunit of signal peptidase complex
PBS2	Q60*	MAP kinase kinase of the HOG signaling pathway
URA2	F1447L	Bifunctional carbamoylphosphate synthetase
MAL11	S317Y	High-affinity maltose transporter
RRP8	Q148K	Nucleolar rRNA methyltransferase
AQY1	I99T	Spore-specific water channel
SRP102	D117N	Signal recognition particle (SRP) receptor
GFD2	insA (791nt)	Protein of unknown function
MKT1	A297S	Protein that forms a complex with Pbp1p
Telomer (cm001533)	R103Q	hypothetical protein
Telomer (cm001533)	F38S	hypothetical protein
Telomer (cm001533)	D43E	hypothetical protein

Table 1. Mutations in coding regions in DS71054-evoB, DS71054-evo4 and DS71054-evo6 versus DS71054. Depicted in **bold** the Hxt36/37 N367I mutation and underlined the mutations in Pbs2 in DS71054-evo4 and DS71054-evo6.

		DS68616		CEN.PK113-7D + DS71054 evo6	
		AVG	Std	AVG	Std
Residual sugar	(g/l)	**8.76**	1.00	**4.58**	0.07
Q D-glucose *	(g D-glc/gDW.h)	**0.877**	0.041	**0.661**	0.015
Q D-xylose *	(g D-xyl/gDW.h)	**0.128**	0.007	**0.330**	0.007
Y ethanol	(g EtOH/g sugar)	**0.372**	0.007	**0.386**	0.004
Y glycerol	(g Gly/g sugar)	**0.051**	0.001	**0.045**	0.002
Y acetic acid	(g AA/g sugar)	**0.0039**	0.0003	**0.0039**	0.0001
Y biomass	(gDW/g sugar)	**0.0923**	0.0004	**0.0866**	0.0034

* The D-glucose and D-xylose conversion rates (Q) were calculated from 4 to 10 hours

Table 2. Overview of the fermentation parameters extracted from the anaerobic fermentation of DS68616 and the mixed co-fermentation of CEN.PK113-7D together with the hexokinase deletion strain DS71054-evo6 on mineral medium supplemented with 7 % D-glucose and 3 % D-xylose